

Modulation of C^m/T, G/A, and G/T Triplex Stability by Conjugate Groups in the Presence and Absence of KCl

Howard B. Gamper, Jr.,^{*,‡} Igor V. Kutyavin,[‡] Rebecca L. Rhinehart,[‡] Sergei G. Lokhov,[§] Michael W. Reed,[‡] and Rich B. Meyer^{*,‡}

Epoch Pharmaceuticals, Inc., 1725 220th Street SE, #104, Bothell, Washington 98021, and Novosibirsk Institute of Bioorganic Chemistry, pr. Lavrentjeva 8, Novosibirsk 630090, Russia

Received June 5, 1997; Revised Manuscript Received August 20, 1997[⊗]

ABSTRACT: Apparent equilibrium association constants were determined by gel mobility shift analysis for triple strand formation between a duplex target containing a 21 base long A-rich homopurine run and several end-modified C^m/T (pyrimidine motif; C^m = 5-methylcytosine), G/A (purine motif), and G/T (purine-pyrimidine motif) triplex-forming oligonucleotides (TFOs). Incubations were carried out for 24 h at 37 °C in 20 mM HEPES, pH 7.2, 10 mM MgCl₂, and 1 mM spermine. The purine motif triplex was the most stable ($K_a = 6.2 \times 10^8 \text{ M}^{-1}$) even though the TFO self-associated as a linear duplex. Conjugation of a terminal hexanol or cholesterol group to the G/A-containing TFO reduced triplex stability by 1.6- or 13-fold, whereas an aminohexyl group or intercalating agent (acridine or psoralen) increased triplex stability by 1.3- or 13-fold. These end groups produced similar effects in C^m/T and G/T triplexes, although the magnitude of the effect sometimes differed. Addition of 140 mM KCl to mimic physiological conditions decreased stability of the G/A triplex by 1900-fold, making it less stable than the C^m/T triplex. The inhibitory effect of KCl on G/A triplex formation could be partially compensated for by conjugating the TFO to an intercalating agent (30–350-fold stabilization) or by adding the triplex selective intercalator coralyne (1000-fold stabilization). Although the G/T triplex responded similarly to these agents, the stability of the C^m/T triplex was unaffected by the presence of coralyne and was only enhanced 1.4–2.8-fold when the TFO was linked to an intercalating agent. In physiological buffer supplemented with 40 μM coralyne, the G/A triplex ($K_a = 3.0 \times 10^8 \text{ M}^{-1}$) was more stable than the C^m/T and G/T triplexes by factors of 300 and 12, respectively.

Short homopurine-homopyrimidine runs in double stranded DNA (≥ 7 –12 bp in length in most studies) can be recognized sequence specifically by triplex-forming oligodeoxynucleotides (TFOs)¹ which hydrogen bond to purine bases in the major groove of the duplex [for recent reviews, see Plum et al. (1995); Radhakrishnan and Patel (1994), Sun et al. (1996), Thuong and Helene (1993)]. The ability to recognize unique sequences in DNA has prompted numerous studies on the use of TFOs as agents to modulate gene expression. Short triple-stranded complexes can inhibit transcription initiation if they interfere with the binding of important trans-acting proteins (Cooney et al., 1988). Triplexes formed downstream from a promoter can block transcription elongation if the TFO forms a sufficiently tight complex (Giovannangeli et al., 1996) or is covalently linked to the duplex through an appended reactive group (Duval-Valentin et al., 1992; Young et al., 1991). Reactive TFOs have also been shown to induce targeted mutations in model shuttle vector assays (Havre & Glazer, 1993; Sandor & Bredberg, 1994; Wang et al., 1995). Collectively, these studies indicate that with further development TFOs might

be used in cells to physically block gene expression or to induce mutations for the purposes of gene knockout or correction.

Three motifs have been described for the recognition of homopurine runs by triplex-forming oligodeoxynucleotides. Pyrimidine (C/T) motif TFOs bind parallel to the homopurine run and form T-A-T and C-G-C triplets (Moser & Dervan, 1987). The stability of C/T motif triplexes is sensitive to pH because the cytosine bases of the TFO can only form Hoogsteen bonds when protonated. This motif is used with A-rich homopurine runs, since runs of C-G-C triplets destabilize the triplex at pH 7. 5-Methylcytosine (C^m) is frequently substituted for cytosine because it promotes protonation of the N-3 position (Lee et al., 1984; Povsic & Dervan, 1989). Purine (G/A) motif TFOs bind antiparallel to the homopurine run and form A-A-T and G-G-C triplets (Beal & Dervan, 1991; Pilch et al., 1991). This motif is normally used to target G-rich homopurine runs since the A-A-T triplet has low stability (Howard et al., 1995). Purine-pyrimidine (G/T) motif TFOs, which form T-A-T and G-G-C triplets, are also used to target G-rich homopurine runs (Durland et al., 1991). The relative polarity of the purine-containing strands in this triplex depends upon the number of GpA and ApG steps in the homopurine tract (Sun et al., 1991). An antiparallel orientation is favored by a high number of steps, while a parallel orientation is favored by a low number of steps. In one instance, a homopurine run was successfully targeted using a TFO which contained C, T, and G. This mixed motif TFO bound parallel to the

* Corresponding author. Tel.: (425) 485-8566. Fax: (425) 486-8336.

[‡] Epoch Pharmaceuticals.

[§] Novosibirsk Institute of Bioorganic Chemistry.

[⊗] Abstract published in *Advance ACS Abstracts*, November 15, 1997.

¹ Abbreviations: TFO, triplex-forming oligonucleotide; HEPES, 2-[4-(2-hydroxyethyl)-1-piperazinyl]ethanesulfonic acid; ODN, oligonucleotide; CPG, controlled pore glass; HPLC, high performance liquid chromatography; CD, circular dichroism; HLA, human-leucocyte-associated.

homopurine run and employed a G repeat to hydrogen bond to a run of Gs in the homopurine run (Giovannangeli et al., 1992).

Stability of oligomeric triplexes can be modulated by a variety of agents. The high negative charge density of triple stranded complexes makes them especially sensitive to counterions. The stability of C/T triplexes is linked to the valency of counterions in the order spermine⁴⁺ > Mg²⁺ > K⁺ (Singleton & Dervan, 1993). Furthermore, in a mixed-valence salt solution containing all three counterions, potassium ion is destabilizing. While similar analyses have not been performed with G/A and G/T triplexes, their formation usually requires the presence of Mg²⁺ (Beal & Dervan, 1991). Intercalating agents such as acridine or psoralen can increase the stability of all three types of triplexes when conjugated to the end of a TFO through linkages of appropriate structure and length (Giovannangeli et al., 1992; Mouscadet et al., 1994; Orson et al., 1994; Sun et al., 1989). Upon triple strand formation, the conjugated group usually intercalates at the junction between triplex and duplex domains. A growing list of triplex-selective intercalators has been described including the benzopyridoindole derivatives BePI (Mergny et al., 1992) and BgPI (Pilch et al., 1993), coralyne (Lee et al., 1993; Moraru-Allen et al., 1997), a series of aryl substituted quinoline derivatives (Chandler et al., 1995; Wilson et al., 1993), selected 2,6-disubstituted aminoanthraquinones (Fox et al., 1995), and the benzopyridioquinoxaline derivative B/PQ-4,3 (Marchand et al., 1996). These positively charged aromatic molecules intercalate into C/T triplexes providing significant stabilization. Recently, intercalation of BePI (Escude et al., 1996) and a naphthylquinoline derivative (Cassidy et al., 1996) into G/T triplexes has been demonstrated. To date, however, no examples have been reported of G/A triplexes being stabilized by such agents.

A complicating factor in the use of some TFOs is their tendency to self-associate. Certain G/T-containing TFOs can form aggregates stabilized by guanine quartets (Olivas & Maher, 1995; Scaria et al., 1992). The stability of these complexes is enhanced by KCl, which in turn can dramatically inhibit triplex formation. Some G/A-containing TFOs can form parallel duplexes in the presence of MgCl₂ (Faucon et al., 1996; Noonberg et al., 1995a,b; Trapane et al., 1996). These structures appear to have low stability and may not interfere with triple strand formation under physiological conditions. Even certain C-rich pyrimidine motif TFOs can form four-stranded intercalated structures (i-motif) at neutrality (Mergny et al., 1995). It is likely that the tendency of any given TFO to self-associate will be sequence dependent.

Our current understanding of triplex formation does not permit an accurate prediction of stability. In fact, comparisons of all three triplex motifs are difficult to find in the literature (Escude et al., 1993; Faucon et al., 1996; Mouscadet et al., 1994; Noonberg et al., 1995; Roy, 1994; Scaria & Shafer, 1996). Clearly the best triplex motif for a given homopurine run will depend upon the sequence and length of the run, the counterions present in the reaction buffer, and the presence if any of free or covalently bound intercalating agents or other ligands. The use of base analogs and modified backbones will also influence stability. Among the unmodified TFOs described to date are a subset of G-rich purine motif TFOs that form triplexes which are more stable than the underlying duplexes (Pilch et al., 1991; Svinarchuk

et al., 1995, 1996). By systematically evaluating the variables listed above, triplexes of similar stability might be formed with homopurine runs containing more balanced A:G ratios.

In the present study, gel mobility shift assays have been used to compare equilibrium triplex formation with a 21 base long slightly A-rich homopurine run found in the human DQB1*0302 allele by C^m/T-, G/A-, and G/T-containing TFOs. Inheritance of this allele predisposes individuals to insulin-dependent diabetes mellitus (Nepom & Erlich, 1991). The homopurine run is notable for containing no more than two consecutive G residues or three consecutive A residues and might be predicted to support triplex formation by all three types of TFOs. Incubations were carried out at 37 °C in a physiological buffer with and without 140 mM KCl using TFOs with terminal hydroxyl, hexanol, aminohexyl, acridine, psoralen, or cholesterol groups. The G/A triplex turned out to be the most stable. Although its stability was dramatically decreased in the presence of 140 mM KCl or NaCl, conjugation of the TFO to acridine or psoralen or addition of coralyne to the buffer partially counteracted the effect of KCl. G/A triplexes were rapidly formed using micromolar concentration of TFO, even though these TFOs self-associated in the presence of MgCl₂. The results of this study show that G/A motif TFOs can form very stable triplexes with an A-rich homopurine run in physiological buffer supplemented with coralyne.

MATERIALS AND METHODS

Synthesis of Modified Oligodeoxynucleotides. Oligodeoxynucleotides (ODNs) were synthesized on an Applied Biosystems Model 394 DNA synthesizer using the 1 μmol protocol supplied by the manufacturer. Standard reagents for the β-cyanoethylphosphoramidite coupling chemistry were purchased from Glen Research. Most 3'-end modifications were incorporated into the ODN at the time of synthesis through the use of specially synthesized controlled pore glass (CPG) supports. The preparation of CPGs derivatized with hexanol, aminohexyl, acridine, or cholesterol have been previously described (Gamper et al., 1993). Phosphoramidite for introduction of the 5'-aminohexyl modification was purchased from Glen Research. Phosphoramidites for introduction of the 5'-hexanol, acridine, and cholesterol modifications were prepared as previously described (Reed et al., 1995). Psoralen was conjugated to the 5' or 3' end of a thiophosphate-bearing ODN using the protocol described by Takasugi et al. (1991). The 3'-thiophosphate group required for this reaction was introduced by the method of Kumar (1993).

After ammonia deprotection, the ODNs were HPLC purified, detritylated if necessary, and precipitated from butanol as previously described (Gamper et al., 1993). Residual triethylammonium acetate was removed by dissolving the ODNs in 1 mL of water and drying in the presence of 3 equiv of sodium bicarbonate. Extinction coefficients were calculated using a nearest neighbor model (Cantor et al., 1970) with correction for the molecular weight and absorbance of conjugated end groups. The purity of ODNs was checked by analytical C₁₈ HPLC and by denaturing polyacrylamide gel electrophoresis. Bands were detected by silver staining. All ODNs used in this study were at least 90% pure.

Thermal Denaturation Measurements. A_{260} versus temperature profiles were determined using a Lambda 2 (Perkin-Elmer) spectrophotometer equipped with a PTP-6 automatic multicell temperature programmer. Solutions containing 2 μ M each of 1, 2, or 3 ODNs were heated at the rate of 0.5 °C/min in 20 mM HEPES, pH 7.2, and supplemented with 10 mM $MgCl_2$ and 0 mM or 140 mM KCl (buffers C and D, respectively). Spermine was omitted as it occasionally promoted the aggregation and precipitation of certain ODN combinations. Prior to melting, samples were denatured at 100 °C and then cooled to the starting temperature over a 10 min period. Melting temperatures (T_m values) were determined from the derivative maxima.

Circular Dichroism. CD spectra were recorded at 15 or 54 °C in a Jasco Model J-600 spectrometer. ODN concentration was 2.5 μ M in water or buffer C. Each spectrum is the sum of four scans recorded at a speed of 20 nm/min and a slit width of 1 nm.

Determination of Triplex Equilibrium Association Constants by Gel Mobility Shift Assay. The duplexes used in these studies were 29 bp long and contained a 21 bp homopurine-homopyrimidine run. The pyrimidine-rich strands of these duplexes were 5'-end labeled by treatment with T4 polynucleotide kinase and [γ - ^{32}P]ATP under standard conditions (Ausubel et al., 1989). Labeled ODN was purified using a Nensorb column (NEN Research Products) and had a specific activity of ~6000 cpm/fmol. Duplexes were formed by annealing the pyrimidine-rich strand with a 4-fold molar excess of complement in 20 mM HEPES, pH 7.2, using an incubation profile of 4 min at 80 °C, 6 h at 37 °C, and overnight at 8 °C. Between uses, the duplex was stored at -20 °C.

Triple strand formation was conducted in capped and siliconized polypropylene microcentrifuge tubes (0.65 mL) at 37 °C for at least 24 h in a final volume of 20 μ L unless otherwise noted. The standard reaction buffer was 20 mM HEPES, pH 7.2, 10 mM $MgCl_2$, 1 mM spermine, and 0 mM or 140 mM KCl (buffers A and B, respectively). The concentration of labeled duplex was kept constant (ranging from 10 pM to 5 nM) while the concentration of TFO was varied (10 pM to 30 μ M). All reactions contained 1 μ M of a mixed sequence 20-mer (5'-ACGCTGAATTCTGCATGCTA) added as a nonspecific carrier. Incubations were conducted in an enclosed incubator to reduce evaporation and condensation. In some experiments buffer B was supplemented with 40 μ M coralyne chloride (Sigma). Aqueous stocks of coralyne (0.4–0.8 mM) were kept wrapped in foil at 4 °C for no longer than 1 month.

Triplexes were detected by nondenaturing gel electrophoresis. Immediately prior to analysis, a 2.5 μ L aliquot of each reaction was mixed with 2.5 μ L of weighting solution (15% Ficoll, 0.25% bromphenol blue, and 0.25% xylene cyanole FF) adjusted to contain the same buffer and salts as the sample. C_m/T triplexes were analyzed in a 10% polyacrylamide gel prepared in 90 mM Tris-OAc, pH 6.0, 1 mM $Mg(OAc)_2$ and run at 80 V for 14 h. G/A and G/T triplexes were analyzed in a 10% polyacrylamide gel prepared in 90 mM Tris-borate, pH 8.0, and 5 mM $MgCl_2$ and run at 200 V for 4 h. The running temperature of both gels (0.15 \times 14 \times 16 cm) was approximately 6 °C. Dried gels were visualized by autoradiography and bands were quantified using a Bio-Rad GS-250 phosphorimager.

Equilibrium association constants were calculated by graphing the fraction of labeled pyrimidine-rich target strand in the triplex state (θ_{app}) versus the concentration of TFO in a semi-log plot (Fried & Crothers, 1981) using data averaged from multiple experiments. The apparent equilibrium association constant for triplex formation ($K_a = [\text{triplex}]/[\text{duplex}][\text{TFO}]$) is equal to the reciprocal of the TFO concentration that gives equal amounts of duplex and triplex, provided that this concentration is substantially greater than the concentration of the pyrimidine-rich target strand and that the TFO does not self-associate. Equilibrium association constants could not be calculated for certain G/T motif TFOs which failed to saturate the target duplex and might be underestimated for certain G/A motif TFOs which formed stable homoduplexes. In this study, TFO titrations were usually repeated once or twice to completely span the region of equivalence. In the final titration, the TFO concentration at the equivalence point was always at least 10-fold greater than the concentration of target duplex. K_a s determined by replicate gel shift experiments differed by less than 10%.

Determination of Triplex Equilibrium Association Constants by Photo-Cross-Linking. TFOs conjugated to a 5'-psoralen group were incubated with labeled 29-mer duplex as described above. The equilibrium mixtures were then irradiated for 5 min at 37 °C in an HRI Model 100 near-UV reaction chamber. This treatment photo-cross-linked the psoralen-bearing TFO to one or both Watson–Crick strands of the triplex. Control experiments demonstrated that cross-linkage was complete after 3 min of exposure and that the photoreaction efficiency varied between triplex motifs. Cross-linked products were electrophoretically resolved in a denaturing 8% polyacrylamide gel and quantified by phosphorimaging the dried gel. Percent cross-linked product was plotted versus TFO concentration in a semi-log format. The concentration of TFO which yielded 50% of maximum cross-linkage was taken as equal to $1/K_a$.

Determination of Rates of Triplex Formation and Dissociation. The rate of triple strand formation was monitored by adding TFOs which contained a 5'-psoralen end group to a limiting amount of labeled 29-mer duplex that contained the target homopurine run. Incubations were conducted at 37 °C in buffers A and B using concentrations of TFO that converted at least 40% of the duplex to triple strand at equilibrium. Aliquots were removed over time, immediately irradiated with near-UV light for 3 min at 37 °C (see above), and stored at 4 °C until electrophoresed in a denaturing 8% polyacrylamide gel. The yield of cross-linked product was determined by phosphorimage analysis of the dried gel.

The rate of triplex dissociation was determined in buffer B at 37 °C by adding a 50-fold molar excess of nonreactive TFO to a preformed triple-stranded complex in which the TFO contained a 3'-psoralen end group. Exchange of TFOs rendered the triplex non-photo-cross-linkable. Following addition of competitor TFO, aliquots were removed over time for irradiation and electrophoretic analysis as described above.

RESULTS

Experimental Design. The first intron of the human HLA DQB1*0302 allele contains a 21 base homopurine run composed of 11 adenines and 10 guanines. This run is depicted in Figure 1A as part of a synthetic 29 bp long duplex

A**A-rich (0302) homopurine run (52% A)**

C/T motif 5'-TTCTCTCTCTCTTTCTCTCTCT
 G/A motif 3'-AAGGAGAGAGGAAAGAGGAGA
 G/T motif 3'-TTGGTGTGTGGTTTGTGGTGT
 0302 duplex 5'-ATATAAGGAGAGAGGAAAGAGGAGACAAA
 3'-TATATTCTCTCTCTCTCTCTCTCTGTTT

B**G-rich homopurine run (62% G)**

C/T motif 5'-TTCCCCCTCCCCTTCCCCCTCT
 G/A motif 3'-AAGGGGAGGGGAAAGGGGAGA
 G/T motif 3'-TTGGGGTGGGGTTTGGGGTGT
 G-rich duplex 5'-ATATAAGGGGAGGGGAAAGGGGAGACAAA
 3'-TATATTCCCCCTCCCCCTTCCCCCTCTGTTT

C

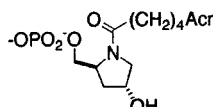
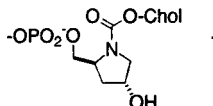
Conjugate Group	3'-Structures	5'-Structures
Hydroxyl	-OH	-OH
Hexanol	-OPO ₂ O(CH ₂) ₆ OH	-OPO ₂ O(CH ₂) ₆ OH
Aminohexyl	-OPO ₂ O(CH ₂) ₆ NH ₃ ⁺	-OPO ₂ O(CH ₂) ₆ NH ₃ ⁺
Psoralen	-OPO ₂ S(CH ₂) ₆ -Pso	-OPO ₂ S(CH ₂) ₆ -Pso
Acridine		-OPO ₂ O(CH ₂) ₄ -Acr
Cholesterol		-OPO ₂ O(CH ₂) ₆ NHCO ₂ -Chol

FIGURE 1: Model systems used in this study. Triplex-forming oligodeoxynucleotides (TFOs) were targeted to two 21 bp long homopurine-homopyrimidine runs. Each run was part of a longer 29 bp duplex. The A-rich homopurine run (panel A) is from the first intron of the human HLA DQβ1*0302 allele (GenBank accession no. K01499). The G-rich homopurine run (panel B) was created by substituting three As in the 0302 sequence with Gs. C^m/T, G/A, and G/T motif TFOs used to target these homopurine runs are aligned above the respective duplexes. Underlined Cs are 5-methyl cytosines. The structures of different groups that were conjugated to the 5' or 3' ends of these TFOs are shown in Panel C.

copied from the 0302 gene. C^m/T, G/A, and G/T motif TFOs specific for this homopurine run are aligned above it. These TFOs were conjugated at either the 3' or the 5' terminus to the groups listed in Figure 1C. Groups tethered to the parallel binding C^m/T motif TFO were positioned at the opposite end of the homopurine run from those tethered to the antiparallel binding G/A and G/T motif TFOs. A concentration series of each TFO was incubated with a limiting amount of synthetic duplex for 24 h at 37 °C in 20 mM HEPES, pH 7.2, 10 mM MgCl₂, 1 mM spermine, and 0 or 140 mM KCl (buffers A and B, respectively). Buffer B approximates the pH and cation composition of the intracellular environment (Alberts, 1989). The fraction of triplex was determined by mobility shift analysis on a nondenaturing polyacrylamide gel, thus permitting determination of the equilibrium association constant.

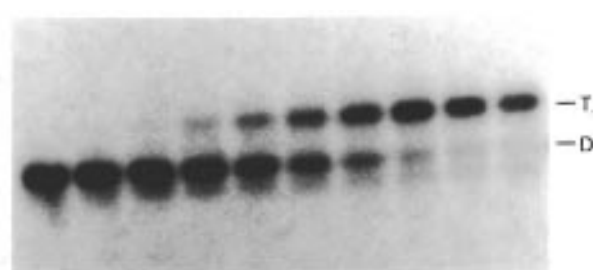
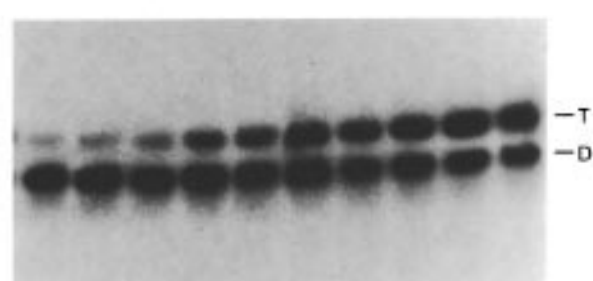
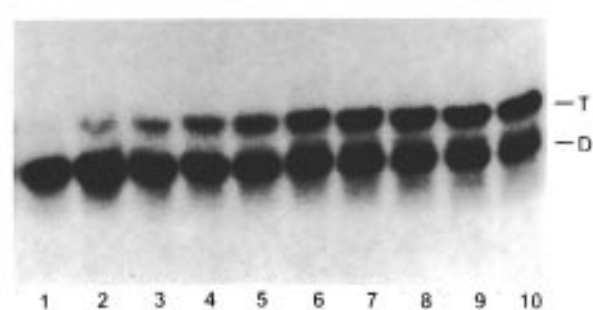
A**B****C**

FIGURE 2: Triple strand formation by unmodified C^m/T, G/A, and G/T motif TFOs targeted to the DQβ1*0302 duplex. A concentration series of each TFO (5'-hydroxyl/3'-hydroxyl) was incubated with labeled 5 nM 0302 duplex in buffer B for 24 h at 37 °C. Reaction aliquots were electrophoresed in the presence of Mg²⁺ and the dried gels were visualized by autoradiography. Panel A, C^m/T motif TFO; panel B, G/A motif TFO; and panel C, G/T motif TFO. TFO concentrations in aliquots applied to lanes 1–10 were 0.06, 0.1, 0.175, 0.3, 0.6, 1, 1.75, 3, 6, and 10 μM (panels A and B) or 0.175, 0.3, 0.6, 1, 1.75, 3, 6, 10, 17.5, and 30 μM (panel C). D = duplex, T = triplex.

To gain insight on how the sequence of the homopurine run alters triplex stability, three As in the 0302 homopurine run were substituted by Gs. Figure 1B shows the synthetic 29 bp long duplex which contains this G-rich homopurine run and the three classes of TFOs used to target it. Like the 0302 target, this homopurine run had too many GpA and ApG steps to permit use of the parallel stranded G/T motif.

The binding isotherms and triplex equilibrium association constants generated by these experiments prompted several additional studies which are included here. Evidence for self-association of G/A motif TFOs was obtained by circular dichroism, gel shift, and *T_m* studies. Additional gel mobility shift assays were conducted to determine how triplex stability is affected by different counterions or by the presence of the triplex selective intercalator coralyne. Finally, rates of triplex formation and dissociation were examined by photo-fixing triplexes which contained a conjugated psoralen group and analyzing for cross-linking by denaturing polyacrylamide gel electrophoresis.

*Determination of Equilibrium Association Constants for Interaction of TFOs with the DQβ1*0302 Homopurine Run.* The results of representative gel mobility shift experiments with unmodified C^m/T, G/A, or G/T motif TFOs are presented in Figure 2. The autoradiograms show that while

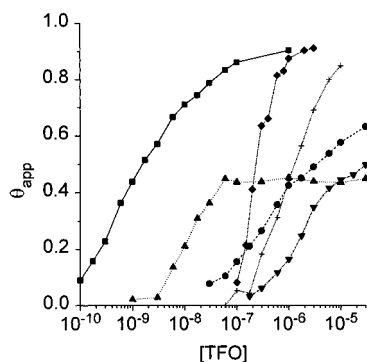


FIGURE 3: Binding isotherms for interaction of unmodified G/A, G/T, and C^m/T motif TFOs with the DQ β 1*0302 duplex in buffers A and B at 37 °C. The fraction of labeled 0302 duplex converted to triplex (θ_{app}) was determined by gel mobility shift analysis. Labeled duplex concentrations were 0.2–5 nM in buffer A and 5 nM in buffer B. Each isotherm is an averaged compilation of data from two or more experiments. G/A motif TFO in buffer A (squares) or B (circles); G/T motif TFO in buffer A (triangles) or B (inverted triangles); and C^m/T motif TFO in buffer A (diamonds) or B (crosses).

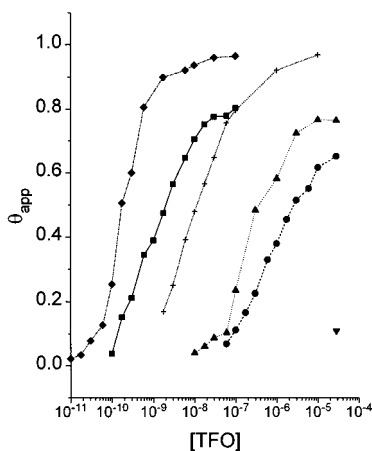


FIGURE 4: Binding isotherms for interaction of end-modified G/A motif TFOs with the DQ β 1*0302 duplex in buffers A and B at 37 °C. G/A motif TFOs with the following end modifications were tested for triplex formation: 5'-aminoethyl/3'-hexanol (squares, buffer A; circles, buffer B), 5'-cholesterol/3'-hexanol (triangles, buffer A; inverted triangle, buffer B), and 5'-acridine/3'-acridine (diamonds, buffer A; crosses, buffer B). Labeled duplex concentrations were 0.02–2 nM in buffer A and 1–5 nM in buffer B.

high concentrations of all three TFOs promoted triplex formation, the pyrimidine motif TFO showed more complete hybridization. The cooperativity of complex formation was clearly greater for the C^m/T motif TFO than for the other two TFOs. Each lane in these gels was analyzed by phosphorimaging to determine the fractional yield of triplex (θ_{app}). These values were then plotted as a function of TFO concentration to give curves such as those in Figures 3 and 4.

It is interesting to compare the duplex-to-triplex titrations in Figure 3, which describe the binding of the same three TFOs to the 0302 duplex in buffers A and B. These titrations spanned five logs of TFO concentration and demonstrate the vastly different stabilities of the triplexes. In the absence of KCl, the order of triplex stability was G/A > C^m/T > G/T. The G/T titration showed nonideal behavior at higher TFO concentrations where the fraction of triplex remained constant. Although this implies that the G/T-containing TFO can self-associate at high concentration, we have been unable to detect such complexes. In the presence of KCl, triplex

stability changed to C^m/T > G/A > G/T. A comparison of the curves obtained in the presence and absence of KCl indicates that the G/A and G/T triplexes were far more sensitive to destabilization by this counterion than the C^m/T triplex. Lastly, regardless of the buffer, the cooperativity of triplex formation (as reflected in the sharpness of the binding curves) was significantly greater for the C^m/T triplex than for the G/A and G/T triplexes.

Figure 4 compares duplex-to-triplex titrations in buffers A and B using three G/A motif TFOs conjugated to different end groups (5'-acridine/3'-acridine; 5'-aminoethyl/3'-hexanol, and 5'-cholesterol/3'-hexanol). In both buffers, triplex stability was dramatically different for the three TFOs. As reported by others (Sun et al., 1989), conjugated acridine groups were highly stabilizing. In contrast, a conjugated cholesterol group was very destabilizing. The combination of a hexanol group and an aminoethyl group conjugated to the TFO-generated triplexes of intermediate stability. Regardless of the end groups, formation of the G/A triplex was significantly inhibited by the presence of KCl.

The trends described above have been quantified by calculating a triplex equilibrium association constant from each titration curve. These constants are compiled in Table 1 for the 0302 homopurine run. Although the G/A triplex was usually the most stable of the three triplex motifs, its stability decreased as much as 4200-fold by the addition of 140 mM KCl. In contrast, the conjugation of an acridine group increased G/A triplex stability (relative to triplexes with 5'-hydroxyl/3'-hydroxyl or 5'-hydroxyl/3'-hexanol end groups on the TFO) by approximately 15-fold in the absence of KCl and by as much as 340-fold in the presence of KCl. Conjugation of two acridine groups instead of one enhanced triplex stability in the presence of KCl and decreased stability in its absence. The effects of other conjugated end groups on G/A triplex stability in buffer A included a 1.6-fold reduction by 3'-hexanol, a 140-fold reduction by 5'-cholesterol, a 560-fold reduction by 3'-cholesterol, and a 1.3-fold enhancement by 5'-aminoethyl. These groups had similar effects in the presence of KCl with the exception of the cholesterol group, which was 50-fold less destabilizing.

Triplex formation with C^m/T motif TFOs was highly cooperative, and the complex was less sensitive to changes of ionic strength or to the addition of end groups. For example, the stability of the C^m/T triplex decreased an average of only 5-fold upon the addition of 140 mM KCl. Conjugated end groups, although exhibiting the same trends described above, altered triplex stability no more than 4-fold in buffer A and 8-fold in buffer B. The cooperativity of C^m/T triplex formation was much greater than observed for the other two triplex motifs. When cooperativity was quantified by determining the logarithm of the difference in TFO concentrations at θ_{app} values of 0.6 and 0.4, the average values for the C^m/T , G/A, and G/T triplexes were 0.11, 0.47, and 0.45 in buffer A and 0.26, 0.86, and 0.49 in buffer B. The isomorphous structure of C^m/T triplexes (Giovannangeli et al., 1992) and the single-stranded character of the corresponding TFOs (data not shown) probably accounts for the high cooperativity observed with this motif. G/A and G/T motif TFOs frequently self-associate, and their triplexes are nonisomorphous (Giovannangeli et al., 1992).

Formation of triplexes between the 0302 homopurine run and G/T motif TFOs was problematic. Several of the TFOs generated nonideal duplex-to-triplex titration curves which

Table 1: Equilibrium Association Constants (K_a) for Triple Helix Formation with the DQ β 1*0302 Homopurine Run in 20 mM HEPES, pH 7.2, 10 mM MgCl₂, 1 mM Spermine, and 0 mM or 140 mM KCl at 37 °C^a

end groups on TFO	C ^m /T motif		G/A motif		G/T motif	
	−KCl	+KCl	−KCl	+KCl	−KCl	+KCl
5′-hydroxyl, 3′-hydroxyl	4.2	0.83	620	0.32	<0.03 ^b	<0.03 ^b
5′-hydroxyl, 3′-hexanol	2.8	0.59	380	0.091	<0.03 ^b	<0.03 ^b
5′-aminohexyl, 3′-hexanol	4.3	0.56	500	0.38	0.30 ^b	<0.03 ^b
5′-acridine, 3′-hexanol	7.7	1.4	5900	31	34	1.8
5′-hydroxyl, 3′-acridine	5.9	0.56	8300	9.1	45	13
5′-acridine, 3′-acridine	3.0	1.0	5300	91	15	8.3
5′-cholesterol, 3′-hexanol	0.83 ^c	0.079	2.8	<0.03	<0.03	NT
5′-hydroxyl, 3′-cholesterol	NT ^c	0.27	1.1	<0.03	1.0 ^b	<0.03

^a The K_a values are multiplied by 10^{−6} M. Equilibria which elicited irregular binding isotherms are denoted as follows in footnotes b and c. ^b At higher concentrations the TFO was unable to drive additional 0302 duplex into the triple-stranded state (e.g., see Figure 3). ^c The pyrimidine rich strand of the 0302 duplex was partially or completely displaced by TFO (e.g., see Figure 8). NT = no triplex.

prematurely plateaued at high TFO concentrations. Conjugation of cholesterol to the TFO usually prevented detectable triplex formation. Only when the TFO was conjugated to an intercalating agent such as acridine was reasonable triplex formation observed. On average, stability of the G/T triplex was decreased 15-fold by the addition of 140 mM KCl.

Validation of the Gel Mobility Shift Assay. Determination of accurate equilibrium association constants by the gel mobility shift technique is predicated on the reaction mixtures actually achieving equilibrium and the electrophoretic analysis not altering that equilibrium. In this context, it was reassuring that the gel shift technique did not show G/A or G/T triplex formation when the incubation buffer lacked MgCl₂. However, the availability of psoralen-conjugated TFOs allowed us to unequivocally verify that both of these conditions were met. When triplexes formed with the 0302 homopurine run were irradiated with near-UV light, psoralen-conjugated TFOs photo-cross-linked to thymidines at the duplex-triplex junction as first described by Takasugi et al. (1991). Depending upon the site of conjugation (5′ or 3′) and the TFO motif (see Figure 1A), irradiation generated both mono- and bis-cross-linked products (reaction at the TpA junction) or just mono-cross-linked product (reaction at the ApC junction). If the pyrimidine-rich strand of the duplex was labeled, the mono- and bis-cross-linked products involving this strand could be resolved and detected in a denaturing polyacrylamide gel thus providing a rapid, noninvasive method for monitoring the rate and extent of triplex formation.

A dilution series of C^m/T, G/A, and G/T motif TFOs each containing a 5′-psoralen group was incubated as usual with the labeled 0302 duplex in buffers A and B. After 24 h at 37 °C, a portion of the reactions were photofixed by irradiation with near-UV light and analyzed by denaturing gel electrophoresis. The other portions were analyzed as usual by the electrophoretic mobility shift assay. A K_a could be determined for each triplex by plotting the percent cross-linked product or the fraction of physical triplex as a function of TFO concentration. These values are presented in Table 2. Both techniques demonstrated that psoralen was equivalent to acridine in stabilizing the C^m/T and G/A triplexes but was 4–8-fold less effective in stabilizing the G/T triplex. The close correspondence between the two sets of data argues that the gel shift technique is accurate. Virtually the same K_a values were obtained when the photo-cross-linking reactions were conducted after 48 h of incubation, indicating that 24 h was sufficient for equilibrium to be attained. A

Table 2: Comparison of Equilibrium Association Constants for Triple Strand Formation with the DQ β 1*0302 Duplex Determined by Gel Electrophoretic Mobility Shift and Psoralen Photo-Cross-Linking Techniques^a

protocol	C ^m /T motif		G/A motif		G/T motif	
	−KCl	+KCl	−KCl	+KCl	−KCl	+KCl
gel shift	7.7 ^b	2.9	4800	32	8.3	0.24
cross-linking	6.2	2.5	7700	22	15	0.22

^a Triple strand formation was conducted in 20 mM HEPES, pH 7.2, 10 mM MgCl₂, 1 mM spermine, and 0 or 140 mM KCl at 37 °C using C^m/T, G/A, and G/T motif TFOs with 5′-psoralen and 3′-hexanol end groups. The K_a values are multiplied by 10^{−6} M. ^b The pyrimidine rich strand of the 0302 duplex was partially displaced by TFO.

limited number of gel mobility shift assays conducted after 48–72 h of incubation also supported this conclusion.

Rates of Formation and Dissociation of the DQ β 1*0302 Triplex. Triple strand formation was monitored at 37 °C by using the photo-cross-linking reaction between 5′-psoralen conjugated C^m/T, G/A, and G/T motif TFOs (0.3 μ M in buffer A and 3 μ M in buffer B) and the 0302 duplex (1 nM) to fix aliquots of the reaction over time. Under these conditions, near equilibrium levels of cross-linkage were obtained after 10 min incubation with all three triplexing motifs in both buffers (data not shown). Reversibility of triplex formation was investigated by monitoring the dissociation of the 0302 triplex formed by a G/A motif TFO with 5′-acridine/3′-psoralen end groups ($K_a = 2.6 \times 10^6$ M^{−1} in buffer B). Photofixation of reaction aliquots at various times after addition of an 8-fold molar excess of a nonreactive G/A motif TFO indicated a first order rate constant of 2.5×10^{-5} s^{−1} for dissociation of the triplex in buffer B ($t_{1/2} = 8$ h; see Figure 5). Under similar conditions, no exchange was observed with a G-rich purine motif triplex incubated for 24 h (Svinarchuk et al., 1994).

Modulation of Triplex Stability by Coralyne. Coralyne is a large planar aromatic molecule which preferentially intercalates between T-A-T triplets in C/T triplexes (Lee et al. 1993; Moraru-Allen et al., 1997). Using the gel mobility shift assay, we investigated whether this agent could stabilize triplexes formed with the 0302 duplex in buffer B. Figure 6 documents the titration of that duplex by unmodified C^m/T, G/A, and G/T motif TFOs in the presence of 40 μ M coralyne. When compared to the binding isotherms generated by the same TFOs in the absence of intercalator (see Figure 3), it is apparent that coralyne significantly enhanced the cooperativity of G/A and G/T triplex formation and stabilized the resultant complexes by approximately 1000-

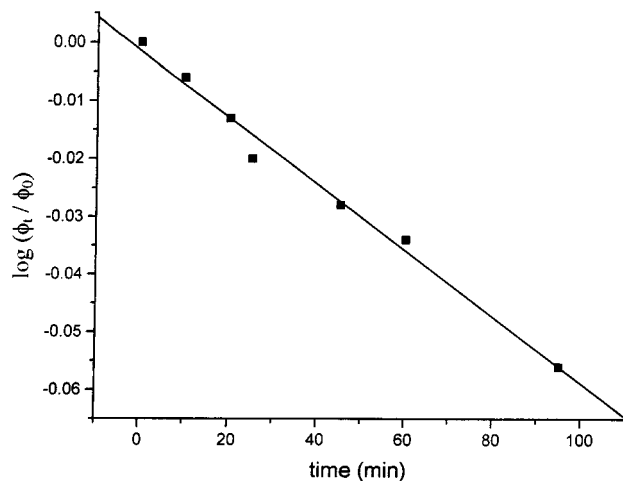


FIGURE 5: Dissociation of a G/A triplex in buffer B at 37 °C. The triplex was preformed by incubating labeled 0302 duplex (20 nM) with G/A motif TFO (5'-acridine/3'-psoralen end groups; 0.125 μ M) for 1 h in buffer B. At time zero competitor G/A motif TFO (5'-acridine/3'-hexanol end groups; 1 μ M final concentration) was added and aliquots were removed over time for irradiation with near-UV light. The yield of photofixed products were determined by denaturing polyacrylamide gel electrophoresis. φ is the fraction of pyrimidine-rich duplex strand photo-cross-linked to TFO. Subscripts 0 and t refer to values of φ ($\varphi_0 = 0.66$) at times 0 and t .

fold. Coralyne improved the cooperativity of C^m/T triplex formation but did not stabilize this complex. Concentrations of 1–4 μ M coralyne provided optimal stabilization of the G/A triplex, while higher concentrations up to 40 μ M were somewhat less effective (Figure 6B). In contrast to coralyne, several naphthylquinoline derivatives failed to stabilize any of the triplexes formed with the 0302 homopurine run (Gamper and Strekowski, unpublished results).

Determination of Equilibrium Association Constants for Interaction of TFOs with the G-Rich Homopurine Run. The G-rich 29 bp duplex was derived from the 0302 duplex by substituting 3 As in the homopurine run with Gs. Equilibrium association constants for interaction of this target with the TFOs listed in Figure 1B were determined by gel mobility shift analysis and are presented in Table 3. Not surprisingly, the C^m/T triplex did not form under any conditions. Runs of G in the target clearly inhibited triple strand formation at neutrality. By contrast, the G/A and G/T triplexes formed in both buffers A and B. This time, however, the G/T triplex was usually the most stable. Addition of 140 mM KCl reduced triplex stability by over 3000-fold for the G/A motif and by nearly 200-fold for the G/T motif. Conjugation of acridine to the TFOs stabilized the G/A triplex but surprisingly destabilized the G/T triplex. With both triplexes, a conjugated intercalating agent reduced the inhibitory effect of KCl. The dramatic differences in triplex stability elicited by changing 3 bases out of 21 in the 0302 homopurine run, shows how sensitive triplex formation can be to changes in base composition. Self-association of these G-rich TFOs, which could influence their ability to form triplexes, was not investigated.

Modulation of G/A Triplex Stability by Counterions. To better understand how counterions influence the stability of the G/A triplex, equilibrium association constants were determined for the interaction of the 0302 duplex with unmodified G/A motif TFO in different buffers at pH 7.2 and 37 °C. The results of this study are summarized in Table

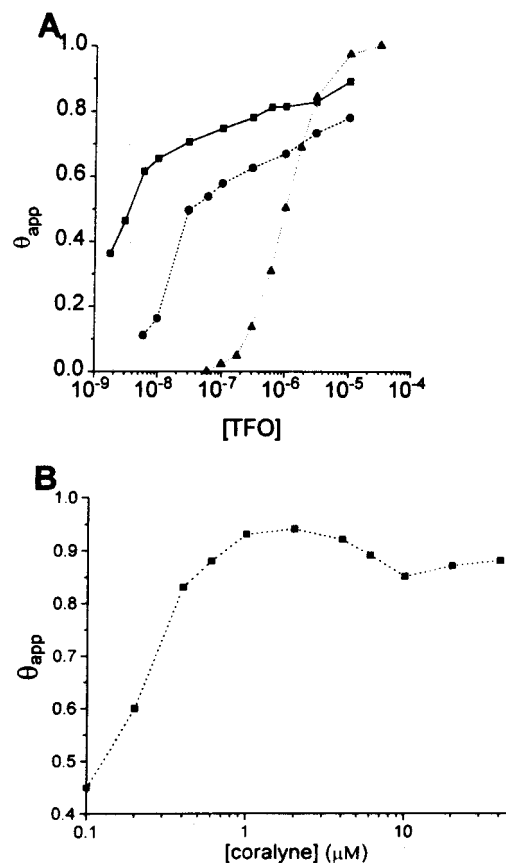


FIGURE 6: Coralyne stabilizes G/A and G/T triplexes but not C^m/T triplex. Labeled 0302 duplex (0.2–1 nM) was incubated with a dilution series of unmodified G/A (squares), G/T (circles), and C^m/T (triangles) motif TFOs in buffer B supplemented with 40 μ M coralyne chloride. After 24 h at 37 °C, the amount of triplex was determined by gel mobility shift analysis. The binding isotherms presented here give triplex equilibrium association constants of 1.0×10^6 M $^{-1}$ (C^m/T motif), 3.0×10^8 M $^{-1}$ (G/A motif), and 2.6×10^7 M $^{-1}$ (G/T motif). (B) Labeled 0302 duplex (4 nM) labeled 0302 duplex was incubated with unmodified G/A motif TFO (100 nM) in buffer B supplemented with the indicated concentrations of coralyne chloride. After 24 h at 37 °C the amount of triplex was determined by gel mobility shift analysis ($\theta_{app} = 0.10$ in the absence of coralyne).

Table 3: Equilibrium Association Constants for Triple Helix Formation with the G-Rich Duplex in 20 mM HEPES, pH 7.2, 10 mM MgCl₂, 1 mM Spermine, and 0 mM or 140 mM KCl at 37 °C^a

end groups on TFO	C^m/T motif		G/A motif		G/T motif	
	–KCl	+KCl	–KCl	+KCl	–KCl	+KCl
5'-hydroxyl, 3'-hydroxyl	NT	NT	110	$\ll 0.03$	480	2.7
5'-acridine, 3'-hexanol	NT	NT	160	0.77 ^b	120	1.8

^a The K_a values are multiplied by 10^{-6} M. NT = no triplex detected.

^b At higher concentrations the TFO was unable to drive additional 0302 duplex into the triple-stranded state.

4. Taking buffer B as the reference point, small changes in spermine concentration dramatically altered triplex stability. When this polyvalent cation was omitted from the buffer, stability was reduced by a factor of 5. By contrast, when its concentration was raised to 5 mM, stability was increased by a factor of nearly 40. MgCl₂ (10 mM) was clearly stabilizing since removal of this divalent cation eliminated triplex formation. Others have noted that the formation of antiparallel triplexes is dependent upon the presence of MgCl₂ or spermine (Beal & Dervan, 1991; Kohwi & Kohwi-Shigematsu, 1988). As mentioned earlier, 140 mM KCl was

Table 4: Counterion Dependence of the Equilibrium Association Constant for G/A Motif Triple Helix Formation with the DQ β 1*0302 Duplex at 37 °C^a

counterion concentration (mM)				K_a ($\times 10^{-6}$ M)
NaCl	KCl	MgCl ₂	spermine	
0	0	10	1	620
140	0	10	1	0.64
0	140	10	1	0.32
0	140	0	1	NT
0	140	10	0	0.062
0	140	10	5	12

^a Triple strand formation using unmodified G/A motif TFO was conducted in 20 mM HEPES, pH 7.2, supplemented with the indicated salts. NT = no triplex detected.

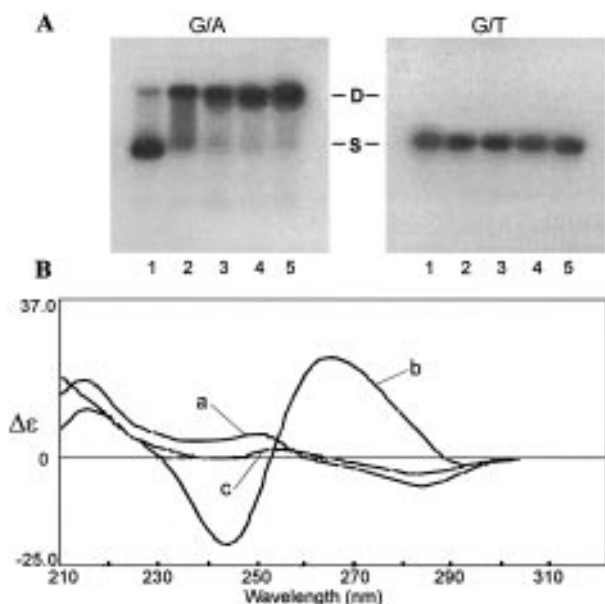


FIGURE 7: G/A motif TFOs targeted to the DQ β 1*0302 homopurine run self-associate as parallel stranded duplexes. (Panel A) Gel retardation analysis of G/A and G/T motif TFOs with 5'-hydroxyl/3'-hexanol end groups. A fixed amount of each 5'-end labeled TFO was added to a dilution series of the same TFO and incubated (without preannealing) for 24 h at 37 °C in buffer B. Aliquots were electrophoresed as for antiparallel triplexes. Autoradiographs of the dried gels are presented. TFO concentrations of aliquots applied to lanes 1–5 were 0.05, 0.3, 3, 30, and 300 μ M. S = single strand, PD = parallel duplex. (Panel B) Circular dichroism spectra of a G/A motif TFO with 5'-hydroxyl/3'-hexanol end groups. Solution conditions were water at 15 °C (spectrum a) and buffer C at 15 °C (spectrum b) or 54 °C (spectrum c).

destabilizing since its elimination from the buffer increased the equilibrium association constant by approximately 1000-fold. Substitution of NaCl for KCl increased the equilibrium association constant by 2-fold. Thus, within the context of buffer B, spermine and MgCl₂ exert a stabilizing influence while KCl and NaCl exert a destabilizing influence. Similar trends have been observed for C/T triplexes (Maher et al., 1990; Singleton & Dervan, 1993).

Self-Association of G/A-Containing TFOs. Some G/A- and G/T-containing TFOs self-associate under physiological conditions (Noonberg et al., 1995a; Olivas & Maher, 1995; Scaria et al., 1992). This possibility was investigated for two representative 0302-targeting TFOs by gel retardation analysis. The autoradiographs in Figure 7A demonstrate that a G/A motif TFO acquired self-structure at high concentration whereas a G/T motif TFO did not. In this particular experiment, the TFOs were incubated in buffer B at 37 °C and then electrophoresed in the presence of 5 mM MgCl₂ at

Table 5: Melting Temperatures of Self-Associated G/A Motif TFO/s^a

end groups on TFO	–KCl	+KCl
5'-hydroxyl, 3'-hydroxyl	37	35
5'-hydroxyl, 3'-hexanol	38	35
5'-hydroxyl, 3'-acridine	42	38
5'-acridine, 3'-acridine	43	41
5'-hydroxyl, 3'-cholesterol	55	67

^a The TFOs were designed to target the DQ β 1*0302 duplex. T_m s (°C) were determined in 20 mM HEPES, pH 7.2, 10 mM MgCl₂, 1 mM spermine, and 0 or 140 mM KCl.

6 °C. Migration of the structured G/A-containing ODN was slightly retarded relative to a Watson–Crick duplex with the same sequence (data not shown). The effect of other counterions including the presence or absence of potassium and spermine in the incubation or gel running buffers was also examined. No self-structure was detected for the G/T motif TFO under any conditions. Conversely, detection of the G/A self-structure required electrophoresis in the presence of MgCl₂ but was unaffected by the composition of the incubation buffer or by addition of other counterions to the gel running buffer. These results can be explained if formation of self-structure is rapid and reversible at 37 °C but less so at 6 °C.

Thermal melting profiles of self-association by G/A motif TFOs conjugated to different end groups were determined by UV absorption spectroscopy. The melting curves showed a single transition with no apparent hysteresis. With one exception, the melting temperatures (T_m s; Table 5) were 37–43 °C in buffer C (no KCl) and 35–41 °C in buffer D (140 mM KCl). A TFO conjugated to cholesterol, however, was significantly more stable. In buffer D, it had a T_m of 67 °C. The marked self-association of this TFO probably accounts for why a conjugated cholesterol group is so inhibitory to G/A motif triplex formation.

The self-structures observed here are most likely parallel stranded duplexes composed of G–G and A–A base pairs. This type of complex has been described for other G/A-containing TFOs (Faucon et al., 1996; Noonberg et al., 1995a,b; Porumb et al., 1996; Trapane et al., 1996). The circular dichroism of these duplexes is characterized by negative and positive peaks at 244 and 263 nm, respectively (Rippe et al., 1992). In this study, the same peaks were observed when the CD spectrum of a G/A motif TFO was recorded at 15 °C in buffer C but not when the temperature was increased to 54 °C or the buffer replaced with water (Figure 7B). Recently, we experimentally verified the parallel orientation of strands in the 0302 G/A homoduplex by mapping alkylation sites induced in one strand of the duplex when a chlorambucil group was conjugated to the 3'-end of the other strand (Lampe et al., 1997).

Strand Displacement Activity of C^m/T-Containing TFOs Conjugated to Cholesterol and Psoralen. Figure 8 illustrates representative gel mobility shift patterns obtained when the 0302 duplex was incubated in buffer A with increasing concentrations of C^m/T motif TFOs bearing a cholesterol or psoralen end group. As the TFO concentration was raised, the labeled pyrimidine-rich strand of the duplex was driven into two bands corresponding to triple-stranded and single-stranded species. Displacement of the pyrimidine-rich strand from the 0302 duplex was favored by absence of KCl and required both a high concentration of TFO and its conjugation to a cholesterol or psoralen end group. The putative

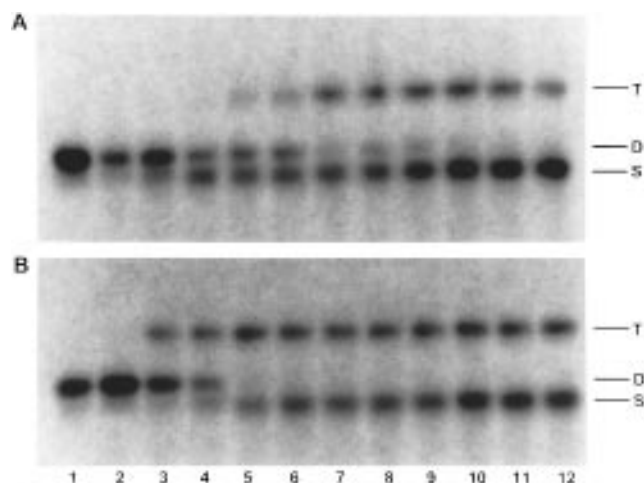


FIGURE 8: C^m/T motif TFOs conjugated to cholesterol or psoralen have strand displacement activity in buffer A. 0302 duplex (5 nM) (pyrimidine-rich strand labeled) was incubated in buffer A with dilution series of G/A motif TFOs containing (A) 5'-cholesterol/3'-hexanol or (B) 5'-psoralen/3'-hexanol end groups. After 24 h at 37 °C, aliquots were analyzed for triplex formation as usual. TFO concentrations of aliquots applied to lanes 1–12 were 0, 0.1, 0.3, 0.6, 0.8, 1.0, 1.25, 1.5, 1.75, 3, 6, and 10 μ M (panel A) or 0, 0.06, 0.1, 0.175, 0.3, 0.4, 0.6, 1, 1.75, 3, 6, and 10 μ M (panel B). S = single strand, D = duplex, T = triplex.

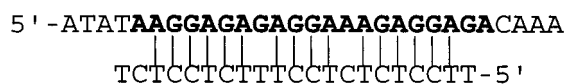


FIGURE 9: Mismatched duplex formed by strand displacement activity of C^m/T motif TFOs linked to cholesterol or psoralen. Conjugated end groups are not shown.

antiparallel duplex is 18 bp long and has two mismatches (Figure 9). In buffer C, this mismatched duplex had a T_m of 58 °C when linked to a cholesterol group. By comparison, the perfect 0302 duplex had a T_m of 66 °C, and the mismatched duplex with no conjugated cholesterol or psoralen group had a T_m of 52 °C. In both examples, the displaced pyrimidine-rich strand predominated at higher TFO concentrations, thus indicating that the mismatched duplex was more stable than the triplex. We surmise that a conjugated psoralen or cholesterol group contributes to strand displacement by hydrophobically interacting with the purine-rich overhang of the mismatched duplex. The strand displacement reaction described here is a natural consequence of the reduced sequence complexity of TFOs and could be avoided by using a longer DNA target.

DISCUSSION

Triplex equilibrium association constants were determined for the interaction of a naturally occurring 21 base long A-rich homopurine run with C^m/T , G/A, and G/T motif TFOs conjugated to different end groups. Triple strand formation was conducted in a physiological buffer (buffer B) at 37 °C or in the same buffer without KCl (buffer A). Under both conditions, G/A motif TFOs formed the most stable triplexes with K_{as} as high as $8.3 \times 10^9 \text{ M}^{-1}$ in buffer A and $3 \times 10^8 \text{ M}^{-1}$ in buffer B. These equilibrium association constants were achieved by conjugating an acridine group to the TFO or by adding coralyne to the buffer. In contrast, the most stable C^m/T and G/T triplexes had K_{as} 1–3 orders of magnitude smaller. These results extend the repertoire of homopurine runs recognized by A/G motif TFOs in physiological conditions and suggest that in the presence of

coralyne, homopurine runs with even higher A content could be addressed.

Traditionally, G/A motif TFOs have been targeted to G-rich homopurine runs where they sometimes form triplexes that are more stable than the underlying duplexes (Pilch et al., 1991; Svinarchuk et al., 1995, 1996). Hence, the strong binding reported here to an A-rich homopurine run is unusual, given that the A-A-T triplet may be much less stable than the G-G-C triplet (Howard et al., 1995). It is possible that the G/A triplex is frayed at one or both ends in buffer B, thus eliminating up to three A-A-T triplets and creating a complex rich in G-G-C triplets. Low cross-linking efficiencies of chlorambucil-bearing G/A motif TFOs targeted to the same homopurine run as described here are consistent with this possibility (Lampe et al., 1997). However, this study also showed that cross-linking becomes very efficient when the TFO is conjugated to an intercalating agent or the buffer is supplemented with coralyne or lacks KCl. Thus, the significant stabilization of G/A triplexes under these conditions may be partially attributable to an elimination of fraying.

A review of the equilibrium association constants in Tables 1–4 shows that relative stability of the three types of triplexes can change depending upon incubation conditions, the presence of conjugated end groups, and the sequence of the homopurine run. For example, while all three triplexes were similarly affected by the addition of 140 mM KCl to the buffer or by the conjugation of various end groups to the TFO, the magnitude of these effects was often quite different for each triplex. In a similar vein, substitution of just three As in the 0302 homopurine run by Gs (to create three repeats of four guanines each) dramatically altered the stability of all three triplex motifs. The ratio of G to A, the number of GpA and ApG steps, and the length of base repeats in the homopurine run are known to modulate triple strand formation. The inability to reliably predict how these and other changes alter triplex stability underscores the usefulness of systematically comparing the three triplexing motifs with additional homopurine runs. Such studies are infrequent in the literature and have not usually employed a physiological buffer.

The marked sensitivity of G/A triplexes to changes in monovalent cation concentration is distinctive among the three motifs. Cooperativity and stability were significantly reduced in the presence of 140 mM KCl or NaCl. Molecular mechanics simulations suggest that the phosphates of the TFO and the purine-rich strand of the target are much closer to one another in a G/A triplex than in a C/T triplex (Laughton & Neidle, 1992). This could amplify response of the G/A triplex to changes in salts. Table 5 demonstrates that the G/A triplex is stabilized by spermine and Mg^{2+} and destabilized by K^+ and Na^+ in a mixed valence salt solution. The significant drop in stability induced by adding NaCl or KCl to the buffer is probably due to displacement of Mg^{2+} and spermine counterions from the triplex by the added univalent cation (Singleton & Dervan, 1993). Our T_m studies showed that promotion of parallel G/A duplex formation is not a factor here since KCl does not stabilize this structure.

The G/A motif TFO is also unique in the degree to which conjugation of an intercalating agent stabilized triplex formation with the 0302 duplex in physiological buffer. Under these conditions, the unmodified G/A triplex was 3-fold less stable than the C^m/T triplex. Upon conjugation of a single 5' acridine group, however, the G/A triplex

became 20-fold more stable than the C^m/T triplex. Since the binding energy of an intercalated ligand is probably similar for the two types of triplexes, differential stabilization of the G/A triplex may be indicative of greater cooperativity in the binding of TFO and intercalating agent to DNA. The acridine group probably acts as a molecular anchor reducing the probability of TFO dissociation from the duplex. With the 0302 target, this stabilizing mechanism is more important for the G/A and G/T triplexes than the C^m/T triplex.

Other conjugated ligands generally had similar effects on the three classes of triplexes. Hexanol and aminohexyl groups are often appended to ends of ODNs as a way to confer resistance to exonucleases (Gamper et al., 1993). The aminohexyl group also functions as a convenient site for postsynthetic modification. Our study shows that neither group substantially altered triplex stability. In contrast, the cholesterol moiety was uniformly inhibitory to triplex formation when linked to a TFO. This ligand abolished binding by the G/T motif TFO, promoted strand displacement by the C^m/T motif TFO, and stabilized self-association of the G/A motif TFO. In the past, cholesterol has been conjugated to ODNs as way to improve cellular uptake (Boutorine et al., 1992; Ing et al., 1993; Krieg et al., 1993). Our results provide another reason why this strategy should allow for release of cholesterol from the TFO once internalization has taken place (Oberhauser & Wagner, 1992; Vu et al., 1994). Of note is the variable effect of adding two acridine moieties to a TFO instead of just one. Depending upon whether KCl was present or not, the additional intercalator could be beneficial or inhibitory to triplex formation. The latter effect may reflect interaction of the two acridines with each other in the uncomplexed TFO.

Coralyne is a positively charged aromatic heterocycle which stabilizes poly[d(TC)]·poly[d(GA)]·poly[d(C⁺T)] at low ionic strength and pH 7 by possibly intercalating between every base triad (Lee et al., 1993). In this work, coralyne enhanced the cooperativity of triple strand formation in physiological conditions, especially for the G/A and G/T triplexes. It also increased the stability of the antiparallel triplexes by 1000-fold, probably due to intercalation between base triads possibly without regard to neighbor exclusion. While each such event will provide binding energy, intercalation of this agent between triplets formed at GpA and ApG steps in the underlying homopurine run may provide the greatest stabilization. Since such triplets are nonisomorphic in antiparallel triplexes (Giovannangeli et al., 1992), intercalation at these sites may reduce the stress due to distortion and provide additional stacking energy. Enhancement of G/A triplex formation by coralyne is the first report of this motif being stabilized by a triplex-selective intercalator. The stabilizing effect appears to be greater in buffer B than in buffer A and is not totally additive with respect to that induced by a conjugated acridine group (Lampe et al., unpublished results). Studies are underway to determine the breadth of G/A and G/T triplexes which are stabilized by coralyne. Although the C^m/T triplex formed with slightly greater cooperativity in the presence of coralyne, its stability was unchanged. Weak stabilization of other short C/T triplexes by coralyne has recently been described (Escude et al., 1995). The binding affinity of coralyne for these triplexes is reduced by the presence of positively charged C-G-C triplets (Moraru-Allen et al., 1997).

If a TFO self-associates, its ability to form a triplex can be compromised. Although G/A motif TFOs targeted to the

0302 homopurine run formed parallel duplexes, significant inhibition of triple strand formation was only observed when the self-structure was very stable. Such was the case when cholesterol was conjugated to the TFO. Self-association of two such TFOs positions the cholesterol groups adjacent to one another at one end of a parallel duplex and provides significant additional binding energy. Several G/T motif TFOs targeted to the 0302 homopurine run failed to drive triplex formation to completion. This effect is probably attributable to some form of self-aggregation which can occur in the absence of KCl. The A-rich character of the TFO and the absence of long runs of G argue against G-quartet formation. By increasing affinity for the target duplex, conjugation of an intercalating agent to the TFO allowed triple strand formation to take place at concentrations below those which favored aggregation. It is not clear why aggregation of G/T motif TFOs was not detected by thermal melting and gel retardation experiments. In a recent study of a G-rich G/T motif TFO, no signs of higher order structure could be detected by gel retardation analysis even though other lines of evidence suggested self-association (Vasquez et al., 1995).

Strand displacement may represent an alternative to triplex formation between the synthetic 0302 duplex used here and some G/A-containing TFOs. This reaction was observed with certain C^m/T-containing TFOs and resulted in the formation of a mismatched duplex with the purine-rich strand of the 0302 target. G/A motif TFOs could form an analogous complex with the pyrimidine-rich strand of the same target. It is conceivable that this type of complex may not have been resolved from the 0302 duplex during electrophoresis. If so, strand displacement could be an additional reason why some G/A motif TFOs failed to drive triplex formation to completion.

In the presence of coralyne the, G/A triplex described here has sufficient stability in physiological buffer to warrant targeting of the 0302 allele in permeabilized human cells by reactive derivatives of the G/A motif TFO. Since this TFO targets an intron, inhibition of transcription would be best achieved by cross-linking the TFO to the target sequence. Use of a conjugated psoralen group is problematic in the presence of 1–2 μ M coralyne due to near UV absorption by the latter. We have previously described covalent linkage of a C^m/T motif TFO bearing a terminal chlorambucil group to double-stranded DNA (Kutyavin et al., 1993). G/A motif TFOs bearing this same group cross-link to the pyrimidine-rich strand of the 0302 duplex with up to 54% efficiency in physiological buffer (Lampe et al., 1997). Using a chlorambucil-bearing TFO targeted to the 0302 allele in permeabilized human cells, we hope to demonstrate triplex formation with this single copy allele.

ACKNOWLEDGMENT

We thank A. David Adams, Debbie Lucas, and En-jia Yang for preparation of oligonucleotides, Dr. Alexander Gall for the synthesis of 5-(6-iodohexyloxy)psoralen, and Dr. Scot W. Ebbinghaus for critical reading of the manuscript.

REFERENCES

- Alberts, B. (1989) *Molecular Biology of the Cell*, p 304, Garland, New York.
- Ausubel, F. M., Brent, R., Kingston, R. E., Moore, D. D., Seidman, J. G., Smith, J. A., & Struhl, K. (1989) in *Current protocols in molecular biology*, John Wiley, New York.
- Beal, P. A., & Dervan, P. B. (1991) *Science* 251, 1360–1363.

- Boutorine, A. S., Boiziau, C., Le Doan, T., Toulme, J. J., & Helene, C. (1992) *Biochimie* 74, 485–489.
- Cantor, C. R., Warshaw, M. M., & Shapiro, H. (1970) *Biopolymers* 9, 1059–1077.
- Cassidy, S. A., Strekowski, L., & Fox, K. R. (1996) *Nucleic Acids Res.* 24, 4133–4138.
- Chandler, S. P., Strekowski, L., Wilson, W. D., & Fox, K. R. (1995) *Biochemistry* 34, 7234–7242.
- Cooney, M., Czernuszewicz, G., Postel, E. H., Flint, S. J., & Hogan M. E. (1988) *Science* 241, 456–459.
- Durland, R. H., Kessler, D. J., Gunnell, S., Duvic, M., Pettitt, B. M., & Hogan, M. E. (1991) *Biochemistry* 30, 9246–9255.
- Duval-Valentin, G., Thuong, N. T., & Helene, C. (1992) *Proc. Natl. Acad. Sci. U.S.A.* 89, 504–508.
- Escude, C., Francois, J.-C., Sun, J.-S., Ott, G., Sprinzl, M., Garestier, T., & Helene, C. (1993) *Nucleic Acids Res.* 21, 5547–5553.
- Escude, C., Nguyen, C. H., Mergny, J.-L., Sun, J. S., Bisagni, E., Garestier, T., & Helene, C. (1995) *J. Am. Chem. Soc.* 117, 10212–10219.
- Escude, C., Sun, J.-S., Nguyen, C. H., Bisagni, E., Garestier, T., & Helene, C. (1996) *Biochemistry* 35, 5735–5740.
- Faucon, B., Mergny, J.-L., & Helene, C. (1996) *Nucleic Acids Res.* 24, 3181–3188.
- Fox, K. R., Polucci, P., Jenkins, T. C., & Neidle, S. (1995) *Proc. Natl. Acad. Sci. U.S.A.* 92, 7887–7891.
- Fried, M., & Crothers, D. M. (1981) *Nucleic Acids Res.* 9, 6505–6525.
- Gamper, H. B., Reed, M. W., Cox, T., Viroso, J. S., Adams, A. D., Gall, A. A., Scholler, J. K., & Meyer, R. B. (1993) *Nucleic Acids Res.* 21, 145–150.
- Giovannangeli, C., Rougee, M., Garestier, T., Thuong, N. T., & Helene, C. (1992a) *Proc. Natl. Acad. Sci. U.S.A.* 89, 8631–8635.
- Giovannangeli, C., Thuong, N. T., & Helene, C. (1992b) *Nucleic Acids Res.* 20, 4275–4281.
- Giovannangeli, C., Perrouault, L., Escude, C., Thuong, N., & Helene, C. (1996) *Biochemistry* 35, 10539–10548.
- Havre, P. A., & Glazer, P. M. (1993) *J. Virol.* 67, 7324–7331.
- Howard, F. B., Miles, H. T., & Ross, P. D. (1995) *Biochemistry* 34, 7135–7144.
- Ing, N. H., Beekman, J. M., Kessler, D. J., Murphy, M., Jayaraman, K., Zendegui, J. G., Hogan, M. E., O'Malley, B. W., & Tsai, M.-J. (1993) *Nucleic Acids Res.* 21, 2789–2796.
- Kohwi, Y., & Kohwi-Shigematsu, T. (1988) *Proc. Natl. Acad. Sci. U.S.A.* 85, 3781–3785.
- Krieg, A. M., Tonkinson, J., Matson, S., Zhao, Q., Saxon, M., Zhang, L.-M., Bhanja, U., Yakubov, L., & Stein, C. A. (1993) *Proc. Natl. Acad. Sci. U.S.A.* 90, 1048–1052.
- Kumar, A. (1993) *Nucleosides Nucleotides* 12, 729–736.
- Kutyavin, I. V., Gamper, H. B., Gall, A. A., & Meyer, R. B. (1993) *J. Am. Chem. Soc.* 115, 9303–9304.
- Lampe, J. N., Kutyavin, I. V., Rhinehart, R., Reed, M. W., Meyer, R. B., Gamper, H. B. (1997) *Nucleic Acids Res.* (in press).
- Laughton, C. A., & Neidle, S. (1992) *Nucleic Acids Res.* 20, 6535–6541.
- Lee, J. S., Woodsworth, M. L., Latimer, L. J., & Morgan, A. R. (1984) *Nucleic Acids Res.* 12, 6603–6614.
- Lee, J. S., Latimer, L. J. P., & Hampel, K. J. (1993) *Biochemistry* 32, 5591–5597.
- Maher, L. J., Dervan, P. B., & Wold, B. J. (1990) *Biochemistry* 29, 8820–8826.
- Marchand, C., Bailly, C., Nguyen, C. H., Bisagni, E., Garestier, T., Helene, C., & Waring, M. J. (1996) *Biochemistry* 35, 5022–5032.
- Mergny, J.-L., Duval-Valentin, G., Nguyen, C. H., Perrouault, L., Faucon, B., Rougee, M., Montenay-Garestier, T., Bisagni, E., & Helene, C. (1992) *Science* 256, 1681–1684.
- Mergny, J.-L., Lacroix, L., Han, X., Leroy, J.-L., & Helene, C. (1995) *J. Am. Chem. Soc.* 117, 8887–8898.
- Moraru-Allen, A. A., Cassidy, S., Alvarez, J.-L. A., Fox, K. R., Brown, T., & Lane, A. N. (1997) *Nucleic Acids Res.* 25, 1890–1896.
- Moser, H. E., & Dervan, P. B. (1987) *Science* 238, 645–650.
- Mouscadet, J.-F., Ketterle, C., Goulaouic, H., Carteau, S., Subra, F., Le Bret, M., & Auclair, C. (1994) *Biochemistry* 33, 4187–4196.
- Nepom, G. T., & Erlich, H. (1991) *Annu. Rev. Immunol.* 9, 493–525.
- Noonberg, S. B., Francois, J.-C., Garestier, T., & Helene, C. (1995a) *Nucleic Acids Res.* 23, 1956–1963.
- Noonberg, S. B., Francois, J.-C., Praseuth, D., Guieysse-Peugeot, A.-L., Lacoste, J., Garestier, T., & Helene, C. (1995b) *Nucleic Acids Res.* 23, 4042–4049.
- Oberhauser, B., & Wagner, E. (1992) *Nucleic Acids Res.* 20, 533–538.
- Olivas, W. M., & Maher, L. J. (1995) *Biochemistry* 34, 278–384.
- Orson, F. M., Kinsey, B. M., & McShan, W. M. (1994) *Nucleic Acids Res.* 22, 479–484.
- Pilch, D. S., Levenson, C., & Shafer, R. H. (1991) *Biochemistry* 30, 6081–6087.
- Pilch, D. S., Martin, M. T., Nguyen, C. H., Sun, J. S., Bisagni, E., Garestier, T., & Helene, C. (1993) *J. Am. Chem. Soc.* 115, 9942–9951.
- Plum, G. E., Pilch, D. S., Singleton, S. F., & Breslauer, K. J. (1995) *Annu. Rev. Biophys. Biomol. Struct.* 24, 319–350.
- Porumb, H., Gousset, H., Letellier, R., Salle, V., Briane, D., Vassy, J., Amor-Gueret, M., Israel, L., & Taillandier, E. (1996) *Cancer Res.* 56, 515–522.
- Povsic, T. J., & Dervan, P. B. (1989) *J. Am. Chem. Soc.* 111, 3059–3061.
- Radhakrishnan, I., & Patel, D. J. (1994) *Biochemistry* 33, 11405–11416.
- Reed, M. W., Lukhtanov, E. A., Gorn, V. V., Lucas, D. D., Zhou, J. H., Pai, S. B., Cheng, Y.-c., & Meyer, R. B. (1995) *J. Med. Chem.* 38, 4587–4596.
- Rippe, K., Fritsch, V., Westhof, E., & Jovin, T. M. (1992) *EMBO J.* 11, 3777–3786.
- Roy, C. (1994) *Eur. J. Biochem.* 220, 493–503.
- Sandor, Z., & Bredberg, A. (1994) *Nucleic Acids Res.* 22, 2051–2056.
- Scaria, P. V., & Shafer, R. H. (1996) *Biochemistry* 35, 10985–10994.
- Scaria, P. V., Shire, S. J., & Shafer, R. H. (1992) *Proc. Natl. Acad. Sci. U.S.A.* 89, 10336–10340.
- Singleton, S. F., & Dervan, P. B. (1993) *Biochemistry* 32, 13171–13179.
- Sun, J. S., Francois, J.-C., Montenay-Garestier, T., Saison-Behmoaras, T., Roig, V., Thuong, N. T., & Helene, C. (1989) *Proc. Natl. Acad. Sci. U.S.A.* 86, 9198–9202.
- Sun, J. S., De Bizemont, T., Duval-Valentin, G., Montenay-Garestier, T., & Helene, C. (1991) *C R Acad. Sci. III* 313, 585–590.
- Sun, J. S., Garestier, T., & Helene, C. (1996) *Curr. Opin. Struct. Biol.* 6, 327–333.
- Svinarchuk, F., Bertrand, J.-R., & Malvy, C. (1994) *Nucleic Acids Res.* 22, 3742–3747.
- Svinarchuk, F., Monnot, M., Merle, A., Malvy, C., & Fermandjian, S. (1995a) *Nucleic Acids Res.* 23, 3831–3836.
- Svinarchuk, F., Paoletti, J., & Malvy, C. (1995b) *J. Biol. Chem.* 270, 14068–14071.
- Svinarchuk, F., Debin, A., Bertrand, J.-R., & Malvy, C. (1996) *Nucleic Acids Res.* 24, 295–302.
- Takasugi, M., Guendouz, A., Chassignol, M., Decout, J. L., Lhomme, J., Thuong, N. T., & Helene, C. (1991) *Proc. Natl. Acad. Sci. U.S.A.* 88, 5602–5606.
- Thuong, N. T., & Helene, C. (1993) *Angew. Chem., Int. Ed. Engl.* 32, 666–690.
- Trapane, T. L., Hogrefe, R. I., Reynolds, M. A., Kan, L. S., & Ts'o, P. O. P. (1996) *Biochemistry* 35, 5495–5508.
- Vasquez, K. M., Wensel, T. G., Hogan, M. E., & Wilson, J. H. (1995) *Biochemistry* 34, 7243–7251.
- Vu, H., Hill, T. S., & Jayaraman, K. (1994) *Bioconjugate Chem.* 5, 666–668.
- Wang, G., Levy, D. D., Seidman, M. M., & Glazer, P. M. (1995) *Mol. Cell. Biol.* 15, 1759–1768.
- Wilson, W. D., Tanius, F. A., Mizan, S., Yao, S., Kiselyov, A. S., Zon, G., & Strekowski, L. (1993) *Biochemistry* 32, 10614–10621.
- Young, S. L., Krawczyk, S. H., Matteucci, M. D., & Toole, J. J. (1991) *Proc. Natl. Acad. Sci. U.S.A.* 88, 10023–10026.